
Unsat Core Prediction through Polarity-Aware Representation Learning over Clause-Literal Hypergraphs

Zhenchao Sun¹ Shuai Ma¹ Ping Lu¹ Chongyang Tao¹

Abstract

Graph neural networks have been widely used in Boolean satisfiability (SAT) tasks to learn structural information from SAT formulas. The goal of these studies is to solve SAT instances or to enhance SAT solvers, including tasks such as unsat-core prediction. However, most existing approaches model a SAT formula as a bipartite graph or a directed acyclic graph, which are less expressive in capturing higher-order interactions among literals and clauses. Moreover, these approaches are limited in modeling intrinsic polarity-related properties of SAT, such as the complementary relationship between the positive and negative literals of a variable. To address these limitations, we propose a polarity-aware representation learning framework over clause–literal hypergraphs. We model SAT formulas as clause–literal hypergraphs augmented with a clause incidence graph to capture higher-order structural interactions. We then introduce a polarity-aware decomposed mechanism that separates variable representations into polarity invariant and equivariant components, explicitly modeling the relationship between positive and negative literals, with the resulting literal representations propagated along the hypergraph structure. We further incorporate a polarity-inversion consistency regularization to reinforce polarity-consistent representations during training. Experimental results on multiple SAT datasets demonstrate the effectiveness of the proposed approach.

1. Introduction

The boolean satisfiability problem (SAT) is a foundational problem in computer science that impacts many research

¹SKLCCSE Lab, Beihang University, Beijing, China. Correspondence to: Shuai Ma <mashuai@buaa.edu.cn>.

fields, such as planning (Büttner & Rintanen, 2005), verification (Vizel et al., 2015), and security (Mironov & Zhang, 2006). This is the first problem that was proven to be NP-complete (Cook, 1971). Over the past decades, significant progress has been made in SAT solving, particularly with the development of conflict-driven clause learning (CDCL) solvers. CDCL solvers are complete and capable of solving large, complex real-world instances (Biere et al., 2021). However, such effectiveness heavily depends on heuristics that rely on human domain expertise.

Recently, many studies have explored learning-based approaches to solve SAT instances or enhance SAT solving (Bünz & Lamm, 2017; Selsam et al., 2019; Amizadeh et al., 2019; Li et al., 2023; Cameron et al., 2020; Selsam & Bjørner, 2019; Shi et al., 2023; Wang et al., 2024). Graph neural networks (GNNs) have demonstrated impressive capability in learning from structured data (Kipf & Welling, 2016; Hamilton et al., 2017), making them well suited for representing SAT formulas and capturing their structural properties. A representative line of work leverages GNNs to guide the heuristics of CDCL solvers by learning structural information from SAT formulas (Selsam & Bjørner, 2019; Shi et al., 2023; Wang et al., 2024). For instance, some studies model SAT formulas as bipartite graphs and predict unsat-core variables, i.e., variables involved in unsatisfiable cores, to guide variable selection in CDCL solvers (Selsam & Bjørner, 2019; Shi et al., 2023). Others predict backbone variables to initialize the phase selection heuristic (Wang et al., 2024), while additional work applies learning-based models to guide other solver heuristics, such as restarts and clause deletion (Liang et al., 2018; Liu et al., 2024).

Although existing studies have demonstrated effectiveness, these learning-based approaches have several limitations. One such limitation is that existing GNN-based SAT models focus on representation learning from graph structures, and overlook intrinsic properties of the SAT formulation. In SAT problems, each variable is associated with a pair of complementary literals with inverse polarity, corresponding to its positive and negative occurrences. However, existing approaches typically treat literals and clauses as independent graph nodes and form variable representations by directly combining positive and negative literal embeddings,

which weakens the modeling of polarity inversion between them (Zhang et al., 2020; Selsam & Bjørner, 2019). Some methods introduce additional edges between complementary literals (Selsam et al., 2019), while others model variables and clauses as nodes, and encode literal occurrences and their polarities via edge labels (Kurin et al., 2020; Li & Si, 2022; Wang et al., 2024). Although these designs enable message passing between literals, they do not explicitly enforce two key constraints: (i) complementary literals of the same variable should share common information, and (ii) their representations should reflect the polarity inversion relationship. How to effectively incorporate these constraints into model design and training remains an open challenge for learning SAT-related representations.

Beyond literal-level constraints, another limitation is that SAT formulas are often modeled as bipartite graphs or directed acyclic graphs, which limits their capacity to capture higher-order literal and clause interactions. On the one hand, each clause contains multiple literals, and assignments to one literal can influence other literals within the same clause, leading to multi-literal dependencies that cannot be fully captured by pairwise connections. On the other hand, clauses also interact with each other, and satisfiability often depends on dependencies among multiple clauses rather than clause pairs, as reflected in unsat cores (Shi et al., 2023). In bipartite graph representations, message passing is restricted to local neighborhoods, making higher-order and long-range dependency modeling rely on deep architectures that may suffer from over-smoothing. Hypergraphs provide a more natural representation for such structures by directly modeling multi-literal clause constraints via hyperedges, and have been adopted in prior work on SAT-related problems (Feng et al., 2019; Chen et al., 2025).

To address these limitations and model higher-order dependencies in SAT formulas, we propose a **polarity-aware** representation learning framework over clause-literal hypergraphs for unSAT core prediction (PASAT). The framework represents SAT formulas as hypergraphs augmented with a clause incidence graph, and employs a polarity-aware decomposed message passing mechanism that separates variable representations into invariant and equivariant components, capturing the relationship between positive and negative literals of the same variable. To further enforce polarity-consistent representations, we introduce a polarity-inversion consistency regularization, which leverages polarity-flipped formulas as an alternative view during training.

Our main contributions are summarized as follows:

- We propose a polarity-aware representation learning framework over hypergraphs for SAT formulas, augmented with a clause incidence graph, to capture higher-order relationships among literals and clauses.

- We introduce a polarity-aware decomposed mechanism that separates invariant and equivariant components of variable representations, enabling effective modeling of the inherent relationship between positive and negative literals of the same variable.
- We develop a polarity-aware consistency regularization, which leverages polarity-flipped formulas as an alternative view to enhance learning for SAT problems.
- Extensive experiments on multiple SAT datasets demonstrate that the proposed approach achieves improved performance on unsat core variable prediction compared with existing baselines.

2. Preliminaries

A Boolean formula ϕ is composed of Boolean variables combined by logical operators. A Boolean variable v_i can take only two values: *true* or *false* (1/0), and the logical operators include conjunction (\wedge), disjunction (\vee), and negation (\neg). A Boolean formula can be converted into conjunctive normal form (CNF), which is a conjunction of clauses, where each clause is a disjunction of literals (Biere et al., 2021). Each literal l is either a Boolean variable v_i or its negation $\neg v_i$, referred to as the positive and negative literals of v_i , respectively. The two literals have opposite polarity. We denote the number of Boolean variables as N and the number of clauses as M , and use $\mathcal{L} = \{l_1, \dots, l_{2N}\}$ to denote the set of all literals and $\mathcal{C} = \{c_1, \dots, c_M\}$ to denote the set of clauses. The goal of the SAT problem is to determine whether there exists an assignment of the variables such that the Boolean formula ϕ evaluates to *true*. If this is the case, the formula is called *satisfiable*; otherwise, it is *unsatisfiable*. A variable is called an unsat-core variable if at least one of its literals appears in an unsatisfiable core.

3. Methodology

In this section, we present our polarity-aware representation learning framework over hypergraphs for SAT formulas. The framework consists of a hypergraph representation with clause-level structure, a decomposed message passing mechanism for variable representations, and a polarity-inversion consistency regularization for training. An overview of the proposed framework is illustrated in Figure 1.

3.1. Hypergraph-Based Representation for CNF.

We propose a hypergraph-based SAT formula modeling method that represents a CNF formula as a hypergraph and incorporates an additional clause incidence graph (CIG) to facilitate message passing among clauses.

Hypergraph Representation for CNF Formulas. A hypergraph is a generalization of a graph in which hyperedges

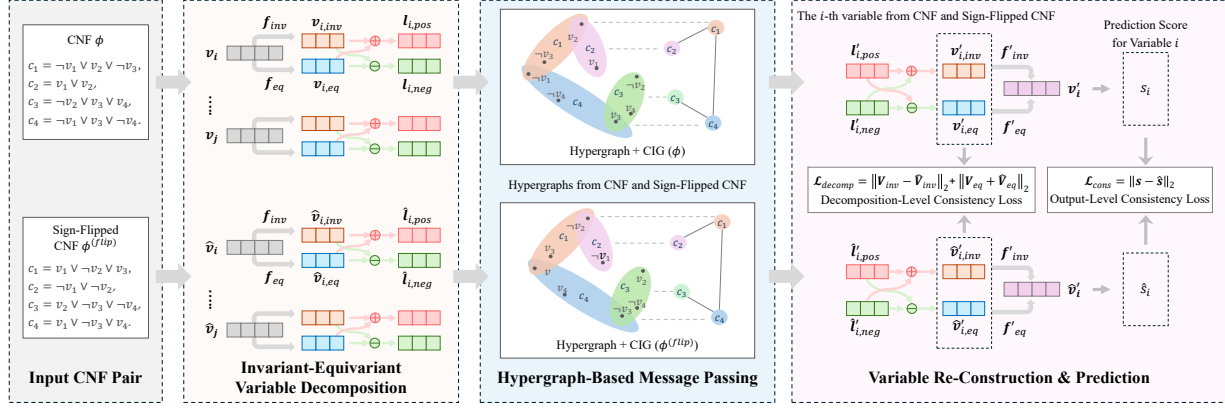


Figure 1. Overview of the proposed polarity-aware hypergraph-based framework (PASAT). Given a CNF formula ϕ , the representation of a variable \mathbf{v}_i is decomposed into a polarity-invariant component $\mathbf{v}_{i,\text{inv}}$ and a polarity-equivariant component $\mathbf{v}_{i,\text{eq}}$. These components are combined to construct positive and negative literal embeddings $\mathbf{l}_{i,\text{pos}}$ and $\mathbf{l}_{i,\text{neg}}$. The literal embeddings are then propagated onto the hypergraph to obtain updated embeddings $\mathbf{l}'_{i,\text{pos}}$ and $\mathbf{l}'_{i,\text{neg}}$. In parallel, a polarity-flipped formula $\phi^{(\text{flip})}$ is processed using shared parameters. The resulting representations from the two views are reconstructed into variable embeddings \mathbf{v}'_i and $\hat{\mathbf{v}}'_i$, which are used to produce prediction scores s_i and \hat{s}_i , with training guided by task supervision and polarity-inversion consistency regularization.

are allowed to connect more than two nodes (Feng et al., 2019). To capture higher-order relationships between literals and clauses, we represent a CNF formula ϕ as a hypergraph $\mathcal{H} = (\mathcal{V}_H, \mathcal{E}_H)$, where \mathcal{V}_H denotes the node set and each node u_i corresponds to a literal l_i . The hyper-edge set \mathcal{E}_H represents clauses in the formula, with each hyperedge e_j corresponding to a clause c_j . An incidence relation is defined such that a node corresponding to literal l_i is connected to hyperedge e_j if l_i appears in clause c_j . This clause–literal relationship is encoded by an incidence matrix $\mathbf{H} \in \mathbb{R}^{2N \times M}$, where N is the number of variables and M is the number of clauses. Specifically, $\mathbf{H}_{ij} = 1$ if literal l_i appears in clause c_j , and 0 otherwise.

In order to model relationships among different clauses, we further extend our representation by constructing a clause incidence graph (CIG), denoted as $\mathcal{G}_C = (\mathcal{V}_C, \mathcal{E}_C)$. Each node $u_j^C \in \mathcal{V}_C$ corresponds to a hyperedge $e_j \in \mathcal{E}_H$, and thus represents the clause c_j in the CNF formula ϕ . Two nodes in \mathcal{V}_C are connected by an edge in \mathcal{G}_C if and only if the corresponding clauses share at least one common literal. Formally, we define the edge weight as $w_{ij}^C = |\mathcal{L}(c_i) \cap \mathcal{L}(c_j)| / |\mathcal{L}(c_i) \cup \mathcal{L}(c_j)|$, where $\mathcal{L}(c_i)$ denotes the set of literals appearing in clause c_i .

Hypergraph-Based Message Passing. Based on \mathcal{H} and \mathcal{G}_C , we design a message passing mechanism that propagates information between literals and clauses while explicitly modeling clause–clause interactions.

Let $\mathbf{L}^{(t)} \in \mathbb{R}^{2N \times d}$ denote the literal representations at message passing round t . Literal–clause message propagation is performed via the incidence matrix $\mathbf{H} \in \mathbb{R}^{2N \times M}$ following the hypergraph convolution formulation in (Bai et al., 2021). Specifically, information is first aggregated from literals to clauses and then propagated back to literals through a

degree-normalized hypergraph operator:

$$\mathbf{M}_H^{(t)} = \mathbf{D}^{-1} \mathbf{H} \mathbf{B}^{-1} \mathbf{H}^\top \mathbf{L}^{(t)} \mathbf{W}^{(t)}, \quad (1)$$

where $\mathbf{W}^{(t)} \in \mathbb{R}^{d \times d}$ is a learnable weight matrix. $\mathbf{D} \in \mathbb{R}^{2N \times 2N}$ and $\mathbf{B} \in \mathbb{R}^{M \times M}$ denote the literal and clause degree matrices, defined as

$$\mathbf{D}_{ii} = \sum_{j=1}^M \mathbf{H}_{ij}, \quad \mathbf{B}_{jj} = \sum_{i=1}^{2N} \mathbf{H}_{ij}. \quad (2)$$

However, this formulation captures clause interactions only implicitly through literals, and thus cannot explicitly model higher-order clause dependencies.

To address this limitation, we extend message passing to the clause incidence graph \mathcal{G}_C . Let $\mathbf{A}_C \in \mathbb{R}^{M \times M}$ denote its weighted adjacency matrix and \mathbf{D}_C its degree matrix. Clause-level message propagation is defined as

$$\begin{aligned} \mathbf{C}^{(t)} &= \mathbf{B}^{-1} \mathbf{H}^\top \mathbf{L}^{(t)} \mathbf{W}^{(t)}, \\ \Delta \mathbf{C}^{(t)} &= \mathbf{D}_C^{-1/2} \mathbf{A}_C \mathbf{D}_C^{-1/2} \mathbf{C}^{(t)} \mathbf{U}, \end{aligned} \quad (3)$$

where $\mathbf{U} \in \mathbb{R}^{d \times d}$ is a learnable weight matrix. The refined clause representations are obtained by

$$\mathbf{C}'^{(t)} = \mathbf{C}^{(t)} + \alpha \sigma(\Delta \mathbf{C}^{(t)}), \quad (4)$$

with a learnable scaling parameter α and a non-linear activation function $\sigma(\cdot)$. The refined clause information is then propagated back to literals by

$$\mathbf{M}^{(t)} = \mathbf{D}^{-1} \mathbf{H} \mathbf{C}'^{(t)}. \quad (5)$$

Finally, each literal representation is updated by combining its current embedding, the aggregated clause message, and the representation of its negated literal:

$$\mathbf{L}^{(t+1)} = f_{\text{update}}(\mathbf{L}^{(t)}, \mathbf{M}^{(t)}, \bar{\mathbf{L}}^{(t)}), \quad (6)$$

where $\bar{\mathbf{L}}^{(t)}$ is a row-wise permutation of $\mathbf{L}^{(t)}$ that provides the embeddings of the corresponding complementary literals. This update function enables the model to jointly capture clause-induced dependencies and polarity-level constraints. By performing multiple rounds of such message passing, the model incrementally integrates higher-order clause structure into the literal representations.

3.2. Invariant–Equivariant Variable Decomposition

While the hypergraph-based message passing mechanism introduced above captures structural dependencies between literals and clauses and generates literal-level representations, we still need to obtain variable-level representations from literal representations. Existing studies usually directly concatenate the positive and negative literal representations and feed them into MLPs to produce variable representations. However, these methods neglect intrinsic properties at the variable level in SAT problems. For example, each pair of complementary literals has opposite polarity. Such polarity relations are independent of clauses and cannot be fully characterized by literal–clause message propagation alone. Moreover, a pair of complementary literals should share certain common information, reflecting the fact that they originate from the same Boolean variable.

To explicitly model this property, we introduce a polarity-aware decomposed message passing mechanism for Boolean variables. This mechanism operates at the variable level and is tightly coupled with the literal-level message passing described in the previous subsection.

Let $\mathbf{V}^{(t)} \in \mathbb{R}^{N \times 2d}$ denote the matrix of variable representations at round t , where each row $\mathbf{v}_i^{(t)} \in \mathbb{R}^{2d}$ corresponds to a Boolean variable v_i . At initialization, all variable representations are set to the same constant vector, i.e., $\mathbf{v}_i^{(0)} = \mathbf{1}_{2d}$ for all $i \in \{1, \dots, N\}$, yielding the initial matrix $\mathbf{V}^{(0)} \in \mathbb{R}^{N \times 2d}$. Each variable representation is decomposed into two d -dimensional components:

$$\mathbf{V}_{\text{inv}}^{(t)} = f_{\text{inv}}^{(t)}(\mathbf{V}^{(t)}), \quad \mathbf{V}_{\text{eq}}^{(t)} = f_{\text{eq}}^{(t)}(\mathbf{V}^{(t)}), \quad (7)$$

where $\mathbf{V}_{\text{inv}}^{(t)}, \mathbf{V}_{\text{eq}}^{(t)} \in \mathbb{R}^{N \times d}$, and $f_{\text{inv}}^{(t)}(\cdot)$ and $f_{\text{eq}}^{(t)}(\cdot)$ are learnable mappings. For variable v_i , its invariant and equivariant components are denoted as $\mathbf{v}_{i,\text{inv}}^{(t)}$ and $\mathbf{v}_{i,\text{eq}}^{(t)}$, respectively. The invariant component encodes polarity-invariant information shared by both literals and captures intrinsic properties of the variable, such as membership in the unsat core. The equivariant component captures polarity-sensitive information that changes sign under Boolean negation.

Based on this polarity-aware decomposition, the representations of the positive and negative literals associated with variable v_i are constructed as

$$\mathbf{l}_{x_i}^{(t)} = \mathbf{v}_{i,\text{inv}}^{(t)} + \mathbf{v}_{i,\text{eq}}^{(t)}, \quad \mathbf{l}_{\neg x_i}^{(t)} = \mathbf{v}_{i,\text{inv}}^{(t)} - \mathbf{v}_{i,\text{eq}}^{(t)}. \quad (8)$$

The literal representation matrix $\mathbf{L}^{(t)} \in \mathbb{R}^{2N \times d}$ can be obtained by stacking all literal vectors. Under this ordering, the positive and negative literals of variable v_i correspond to rows $2i$ and $2i + 1$ in $\mathbf{L}^{(t)}$, respectively. That is,

$$\mathbf{L}_{2i}^{(t)} = \mathbf{l}_{v_i}^{(t)}, \quad \mathbf{L}_{2i+1}^{(t)} = \mathbf{l}_{\neg v_i}^{(t)}. \quad (9)$$

This literal representation matrix serves as the input to the hypergraph-based message passing. After message propagation over the hypergraph and the clause incidence graph, the updated literal representations are denoted as $\mathbf{L}^{(t+1)}$. The variable representations are then recovered by recombining the updated literal representations. For each variable v_i , the invariant and equivariant components are recovered as

$$\begin{aligned} \mathbf{v}_{\text{inv},i}^{(t+1)} &= \frac{1}{2} \left(\mathbf{L}_{2i}^{(t+1)} + \mathbf{L}_{2i+1}^{(t+1)} \right), \\ \mathbf{v}_{\text{eq},i}^{(t+1)} &= \frac{1}{2} \left(\mathbf{L}_{2i}^{(t+1)} - \mathbf{L}_{2i+1}^{(t+1)} \right). \end{aligned} \quad (10)$$

Finally, the variable representation matrix is updated by transforming and concatenating the recovered components:

$$\mathbf{V}^{(t+1)} = [f_{\text{inv}}^{\prime(t)}(\mathbf{V}_{\text{inv}}^{(t+1)}), f_{\text{eq}}^{\prime(t)}(\mathbf{V}_{\text{eq}}^{(t+1)})], \quad (11)$$

where $f_{\text{inv}}^{\prime(t)}(\cdot)$ and $f_{\text{eq}}^{\prime(t)}(\cdot)$ are learnable mappings and $[\cdot, \cdot]$ denotes column-wise concatenation.

3.3. Training Objective

We adopt the same training objective as in prior work on NeuroCore (Selsam & Bjørner, 2019). Specifically, the model is trained to predict a score for each variable, indicating its likelihood of appearing in an unsatisfiable core.

The prediction scores for all variables are produced by applying a linear projection $g(\cdot)$ to the corresponding invariant representations after the final round of message passing (after T rounds)

$$\mathbf{s} = g\left(f_{\text{inv}}^{\prime(T)}(\mathbf{V}_{\text{inv}}^{(T)})\right), \quad (12)$$

Then \mathbf{s} can be passed to the softmax function to define a probability distribution \mathbf{p} over variables.

For each unsatisfiable training instance, the label is given as a binary indicator of whether a variable appears in an unsatisfiable core. Following (Selsam & Bjørner, 2019), we normalize this indicator to obtain a target distribution \mathbf{p}^* by assigning uniform probability to all variables in the core and zero probability to the others. The training objective minimizes the Kullback–Leibler divergence (Kullback & Leibler, 1951) between the target distribution and the predicted distribution,

$$\mathcal{L}_{\text{core}} = D_{\text{KL}}(\mathbf{p}^* \parallel \mathbf{p}) = \sum_{i=1}^N p_i^* \log \frac{p_i^*}{p_i}. \quad (13)$$

This loss encourages the model to assign higher scores to variables that are more likely to participate in an unsatisfiable core, and is optimized jointly with all learnable components of the network.

3.4. Polarity-Inversion Consistency Regularization

In previous sections, we focused on representation learning for SAT formulas and variable-level prediction tasks. We now turn to a training-level constraint motivated by intrinsic properties of SAT problems.

Properties of Literal Polarity Inversion. We first study two intrinsic properties of SAT formulas. Polarity inversion refers to flipping the polarity (sign) of all literals in a CNF formula while preserving the variable set and clause structure. Given a CNF formula $\phi = (x_1 \vee x_2) \wedge (\neg x_3 \vee \neg x_4)$, we invert the polarity of all literals while keeping all logical operations unchanged, obtaining a sign-flipped CNF formula $\phi^{(flip)} = (\neg x_1 \vee \neg x_2) \wedge (x_3 \vee x_4)$. At the variable level, polarity inversion exhibits the following two properties.

Property 1. Given a CNF formula ϕ and its sign-flipped counterpart $\phi^{(flip)}$, the satisfiability of the formula remains unchanged. Moreover, variable-level properties that depend on the structural information of the formula are invariant under polarity inversion. For example, if a set of variables constitutes an unsat-core variable set in an unsatisfiable formula ϕ_{unsat} , the same variables also constitute an unsat-core variable set in $\phi_{\text{unsat}}^{(flip)}$.

Property 2. For properties related to variable assignments, polarity inversion preserves variable identities while flipping their assignments. This property is also exploited in NeuroBack (Wang et al., 2024), which constructs dual formulas by negating all backbone variables in the original formula. The labels of the resulting sign-flipped formulas correspond to the negated phases of the backbone variables.

Polarity-Inversion Consistency for Training. Motivated by the above properties, we introduce a polarity-inversion-based consistency training strategy to encourage the model to learn intrinsic structural properties of SAT problems. For each CNF formula ϕ in the training set, we construct a sign-flipped counterpart $\phi^{(flip)}$ as an alternative view. Both ϕ and $\phi^{(flip)}$ are processed by the same network with shared parameters, producing variable-level predictions for each view, and the standard variable-level prediction loss is applied independently to both views.

To encourage polarity-aware representations, we further introduce a consistency regularization loss between predictions from the two views. This loss enforces polarity-invariant information (*Property 1*) to remain unchanged and polarity-equivariant information (*Property 2*) to transform consistently under polarity inversion. For the unsat-core prediction task, the prediction vectors \mathbf{s} and $\mathbf{s}^{(flip)}$ from ϕ and

$\phi^{(flip)}$ are encouraged to be similar, since polarity inversion does not change unsat-core variables. We denote the corresponding prediction vectors as \mathbf{s} and $\mathbf{s}^{(flip)}$, respectively. The consistency loss is defined as

$$\mathcal{L}_{\text{cons}} = \frac{1}{|\mathcal{V}|} \left\| \mathbf{s} - \mathbf{s}^{(flip)} \right\|_2^2, \quad (14)$$

where $|\mathcal{V}|$ is the number of variables.

In addition to the output-level consistency, we further propose a decomposition-level consistency constraint to explicitly model invariant and equivariant components under polarity inversion, as introduced in Section 3.2.

For each CNF formula, we use the representations from the final message passing round. Under polarity inversion, the invariant components of the original formula ϕ and the flipped formula $\phi^{(flip)}$ are expected to remain similar, while the equivariant components are expected to differ. Accordingly, we define the following consistency loss

$$\mathcal{L}_{\text{decomp}} = \frac{1}{|\mathcal{V}|} \sum_{i \in \mathcal{V}} \left[\left\| \mathbf{v}_{i,\text{inv}}^{(T)} - \mathbf{v}_{i,\text{inv}}^{(T)(flip)} \right\|_2^2 + \left\| \mathbf{v}_{i,\text{eq}}^{(T)} + \mathbf{v}_{i,\text{eq}}^{(T)(flip)} \right\|_2^2 \right]. \quad (15)$$

Combining the above losses, the overall training objective for a single CNF formula is

$$\mathcal{L} = \mathcal{L}_{\text{core}} + \lambda_{\text{cons}} \mathcal{L}_{\text{cons}} + \lambda_{\text{decomp}} \mathcal{L}_{\text{decomp}}, \quad (16)$$

where $\mathcal{L}_{\text{core}}$ denotes the primary variable-level prediction loss, $\mathcal{L}_{\text{cons}}$ and $\mathcal{L}_{\text{decomp}}$ denote the polarity-inversion consistency losses, and λ_{cons} and λ_{decomp} control the strengths of the two regularization terms.

3.5. Combination with SAT Solvers

Finally, we integrate our neural model into CDCL solvers to guide the SAT solving process. Specifically, we follow the NeuroCore (Selsam & Bjørner, 2019) pipeline, where the predicted variable scores are used to periodically overwrite the solver’s variable activity scores during solving. While NeuroCore invokes the neural model multiple times during solving to update these scores, our approach runs the neural model only once before solving and passes the predicted scores to the CDCL solver as additional input. During solving, the variable activity scores are periodically adjusted using the same predicted scores, without re-invoking the neural model, thereby reducing GPU computation overhead. In this way, our integration method can be viewed as an initialization strategy for variable activity scores.

4. Experiment

In this section, we present an experimental analysis of unsat-core prediction to justify the effectiveness of our method.

Table 1. Unsat-core prediction performance on three datasets. Avg. denotes the average performance over available difficulty levels.

DATASET	METHOD	PRECISION				PR-AUC				ROC-AUC			
		EASY	MEDIUM	HARD	AVG.	EASY	MEDIUM	HARD	AVG.	EASY	MEDIUM	HARD	AVG.
SR	GCN	0.845	0.857	0.938	0.880	0.891	0.894	0.961	0.915	0.703	0.715	0.778	0.732
	NEUROCORE	0.865	0.874	0.945	0.895	0.917	0.922	0.974	0.938	0.769	0.789	0.856	0.805
	SATFORMER	0.847	0.859	0.938	0.881	0.895	0.900	0.964	0.920	0.709	0.726	0.787	0.741
	PASAT(OURS)	0.896	0.900	0.956	0.917	0.950	0.953	0.985	0.963	0.839	0.863	0.913	0.872
CA	GCN	0.221	0.147	0.144	0.171	0.305	0.182	0.158	0.215	0.546	0.505	0.502	0.518
	NEUROCORE	0.335	0.191	0.189	0.238	0.443	0.272	0.285	0.333	0.672	0.573	0.571	0.605
	SATFORMER	0.292	0.136	0.126	0.185	0.404	0.186	0.150	0.246	0.616	0.488	0.477	0.527
	PASAT(OURS)	0.424	0.307	0.493	0.408	0.553	0.406	0.575	0.511	0.759	0.666	0.784	0.736
PS	GCN	0.828	0.710	0.681	0.740	0.898	0.766	0.717	0.794	0.787	0.774	0.776	0.779
	NEUROCORE	0.852	0.749	0.721	0.774	0.920	0.809	0.766	0.832	0.826	0.826	0.835	0.829
	SATFORMER	0.840	0.731	0.696	0.756	0.910	0.788	0.735	0.811	0.808	0.801	0.806	0.805
	PASAT(OURS)	0.864	0.775	0.752	0.797	0.930	0.838	0.803	0.857	0.845	0.861	0.880	0.862

4.1. Experimental Settings

Datasets. We use three generated SAT datasets, SR, Community Attachment (CA), and Popularity-Similarity (PS), constructed following G4SATBench (Li et al., 2024). Each dataset is divided into easy, medium, and hard levels. For each level, the training set contains 80,000 SAT and UNSAT instance pairs, while the validation and test sets each contain 10,000 pairs. For unsat-core prediction, we use only UNSAT instances for both training and evaluation, following NeuroCore (Selsam & Bjørner, 2019). Detailed dataset descriptions are provided in Appendix A.

Baselines and Metrics. We follow the unsat-core prediction setting in G4SATBench (Li et al., 2024) and compare our method with representative baselines, including GCN (Kipf & Welling, 2016), NeuroCore (Selsam & Bjørner, 2019), and SATFormer (Shi et al., 2023). Although many studies have explored learning-based methods for guiding SAT solvers (Kurin et al., 2020; Liu et al., 2024; Wang et al., 2024; Tönshoff & Grohe, 2025), these approaches adopt different pipelines and solver configurations. As a result, direct comparisons with these methods are not feasible, since they do not provide comparable intermediate predictions such as unsat-core variables. Models are evaluated using Top- M Precision, PR-AUC, and ROC-AUC, where M denotes the number of unsat-core variables in each instance.

Implementation Details. In our experiments, the number of message-passing rounds on the hypergraph is set to 4. The regularization term λ_{cons} is selected from $[0.1, 0.3]$, and λ_{decomp} is selected from $[0.05, 0.15]$. All baseline methods follow their released implementations with default parameter settings. The full implementation details and hyperparameter configurations are provided in Appendix B.1.

4.2. Experimental Results

We next present our findings.

Exp-1: Comparison with Existing Methods for Unsat-Core Prediction. We first compare the unsat-core predic-

tion performance of our method with that of the baseline models. The results are reported in Table 1.

Across all datasets, our method consistently achieves the best unsat-core variable prediction performance compared with the baseline models on all difficulty splits. On the SR, CA, and PS datasets, our method improves the average Precision by approximately 2.5%, 71.4%, and 3.0% over NeuroCore, respectively. Notably, the CA dataset, on which our method achieves the largest performance gains, is particularly challenging for representation learning. Due to its community structure, the associations between variables and clauses exhibit clear clustering patterns, resulting in a more complex topology than those in the SR and PS datasets. In addition, CA instances typically have a larger clause-to-variable ratio and a smaller unsat-core size, which leads to lower overall performance on this dataset. In contrast, PASAT models SAT formulas as a hypergraph augmented with a clause incidence graph, enabling the model to capture such complex structural information. Moreover, the proposed invariant-equivariant variable decomposition and polarity-inversion consistency regularization explicitly model the relationships between complementary literals. As a result, PASAT achieves the best performance on the CA dataset and exhibits the largest performance gains among all datasets. The improvements in PR-AUC further indicate that our method produces more accurate and stable ranking scores for unsat-core variables. Overall, these experimental results justify the design of our method.

Exp-2: Ablation Study. We conduct an incremental ablation study to evaluate the effectiveness of the components in our framework. Starting from a bipartite-graph baseline based on NeuroCore, we first replace bipartite graph modeling with hypergraph-based message passing, and then incorporate invariant-equivariant variable decomposition and polarity-inversion consistency regularization. Accordingly, we evaluate four configurations with different component combinations: BIPARTITE GRAPH (NEUROCORE), PASAT (HG ONLY), PASAT (HG+DE), and PASAT (HG+DE+REG). Results are reported in Table 2.

Unsat Core Prediction through Polarity-Aware Representation Learning over Clause-Literal Hypergraphs

Table 2. Ablation via incremental integration of hypergraph message passing (HG), invariant–equivariant variable decomposition (DE), and polarity-inversion consistency regularization (REG). Avg. denotes the average performance over available difficulty levels.

DATASET	METHOD	PRECISION				PR-AUC				ROC-AUC			
		EASY	MEDIUM	HARD	AVG.	EASY	MEDIUM	HARD	AVG.	EASY	MEDIUM	HARD	AVG.
SR	BIPARTITE GRAPH (NEUROCORE)	0.865	0.874	0.945	0.895	0.917	0.922	0.974	0.938	0.769	0.789	0.856	0.805
	PASAT (HG)	0.867	0.879	0.947	0.898	0.919	0.927	0.975	0.940	0.768	0.798	0.858	0.808
	PASAT (HG+DE)	0.885	0.894	0.954	0.911	0.940	0.946	0.984	0.956	0.812	0.844	0.906	0.854
	PASAT (HG+DE+REG, FULL)	0.896	0.900	0.956	0.917	0.950	0.953	0.985	0.963	0.839	0.863	0.913	0.872
CA	BIPARTITE GRAPH (NEUROCORE)	0.335	0.191	0.189	0.238	0.443	0.272	0.285	0.333	0.672	0.573	0.571	0.605
	PASAT (HG)	0.335	0.263	0.482	0.360	0.443	0.360	0.564	0.456	0.680	0.626	0.768	0.691
	PASAT (HG+DE)	0.391	0.272	0.486	0.383	0.520	0.367	0.567	0.485	0.721	0.645	0.782	0.716
	PASAT (HG+DE+REG, FULL)	0.424	0.307	0.493	0.408	0.553	0.406	0.575	0.511	0.759	0.666	0.784	0.736
PS	BIPARTITE GRAPH (NEUROCORE)	0.852	0.749	0.721	0.774	0.920	0.809	0.766	0.832	0.826	0.826	0.835	0.829
	PASAT (HG)	0.855	0.756	0.739	0.784	0.923	0.818	0.788	0.843	0.823	0.829	0.863	0.838
	PASAT (HG+DE)	0.859	0.767	0.750	0.792	0.924	0.828	0.800	0.851	0.832	0.851	0.876	0.853
	PASAT (HG+DE+REG, FULL)	0.864	0.775	0.752	0.797	0.930	0.838	0.803	0.857	0.845	0.861	0.880	0.862

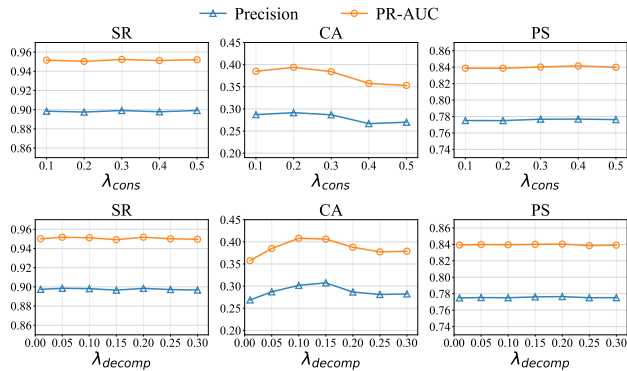


Figure 2. Parameter Analysis.

Across the three datasets, we incrementally build upon a bipartite-graph baseline by adding the components of PASAT, which results in consistent performance improvements on most difficulty splits. On the SR and PS datasets, hypergraph-based message passing already improves performance over the baseline, and the full model further increases Precision by up to 2.5% and 3.0%, respectively. On the CA dataset, the benefits of incremental integration are more pronounced: hypergraph modeling improves the average Precision from 0.238 to 0.360, invariant–equivariant variable decomposition further raises it to 0.383, and the full model reaches 0.408, corresponding to a 71.4% improvement over the baseline. The gains are particularly evident on the Medium and Hard splits, indicating that PASAT effectively captures complex structural patterns and learns from challenging instances with sparse unsat-core variables. Overall, these results demonstrate that each component contributes incrementally to performance improvements.

Exp-3: Parameter Analysis. We analyze two regularization terms, λ_{cons} and λ_{decomp} . We fix $\lambda_{decomp} = 0.05$ and vary λ_{cons} within $[0.1, 0.5]$ with a step size of 0.1. We then fix $\lambda_{cons} = 0.1$ and vary λ_{decomp} within $[0.01, 0.30]$ with a step size of 0.05. All other settings are the same as in Exp-1. Performance is evaluated on the Medium split of each dataset. The results are reported in Figure 2. On the SR and PS datasets, model performance remains relatively

Table 3. Solving results on SAT Competition instances.

DATASET	SOLVER	#SOLVED	#SAT	#UNSAT
SATCOMP 2023	GLUCOSE-DEFAULT	133	59	74
	GLUCOSE-PASAT	148	64	84
SATCOMP 2024	GLUCOSE-DEFAULT	111	50	61
	GLUCOSE-PASAT	118	55	63
SATCOMP 2025	GLUCOSE-DEFAULT	135	60	75
	GLUCOSE-PASAT	141	62	79

stable across different values of both λ_{cons} and λ_{decomp} , indicating low sensitivity to the regularization strength. These datasets exhibit relatively simple structural characteristics, and applying a small amount of regularization is sufficient to obtain strong performance. In contrast, the CA dataset shows clearer performance trends with respect to the two regularization terms. Performance improves when λ_{cons} lies in $[0.1, 0.3]$ and λ_{decomp} lies in $[0.05, 0.2]$. The CA dataset involves more complex variable–clause structures and is more difficult for representation learning, leading to overall lower performance and greater sensitivity to hyperparameter choices. Moreover, larger regularization weights may encourage the model to focus more on polarity-related information, thereby weakening the supervision from the main task and resulting in performance degradation.

Exp-4: Effectiveness of Combination with SAT Solvers.

We evaluate the performance of a CDCL SAT solver combined with our neural model. Specifically, we modify the Glucose solver (Audemard & Simon, 2017) by incorporating the predicted variable scores as additional inputs to guide the solving process. The neural model is trained on instances from the SAT Competition Main Track ¹ between 2017 and 2022, following the same training procedure as NeuroCore (Selsam & Bjørner, 2019). Training details are provided in Appendix B.2. The trained model is then used to generate variable scores for instances from the SATCOMP Main Track in 2023–2025, each of which contains 400 instances. We compare the modified solver with the original Glucose solver under identical configurations. All instances are solved under a time limit of 5000 seconds. The numbers

¹<https://satcompetition.github.io/>

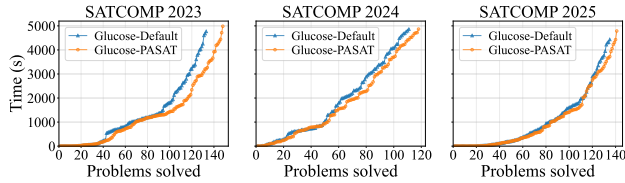


Figure 3. Solving times for SAT Competition instances.

of solved instances are reported in Table 3. On the SATCOMP datasets, Glucose augmented with our method solves more instances overall, outperforming the original Glucose solver by 15, 7, and 6 instances, respectively. Improvements are observed on both SAT and UNSAT instances, indicating that the proposed method provides effective variable-level information for CDCL solving.

In addition, we report cactus plots to illustrate the solving process in Figure 3. Across all datasets, Glucose-PASAT outperforms the default Glucose solver overall. While the two configurations exhibit similar performance on easier instances, Glucose-PASAT demonstrates clear advantages in the medium-to-hard range, where the solving-time curve increases more slowly. These results indicate that the proposed polarity-aware neural guidance provides effective variable-level information that helps the solver navigate difficult search spaces more efficiently.

5. Related Work

In this section, we present the related studies in learning-based approaches for SAT solving.

End-to-End Learning for SAT Solving. A number of studies employ neural networks to solve SAT problems directly (Bünz & Lamm, 2017; Selsam et al., 2019; Amizadeh et al., 2019; Li et al., 2023; Cameron et al., 2020; Chen et al., 2025), most of which formulate SAT solving as a single-bit prediction task for satisfiability. Early work (Bünz & Lamm, 2017) models CNF formulas as bipartite graphs of literals and clauses and applies GNNs for satisfiability classification. NeuroSAT (Selsam et al., 2019) extends this representation by connecting complementary literals and performing message passing between literals and clauses. DG-DAGRNN (Amizadeh et al., 2019) targets circuit SAT by modeling instances as directed acyclic graphs and learning satisfying assignments with gated recursive networks. DeepSAT (Li et al., 2023) represents SAT instances as and-inverter graphs and leverages polarity-aware DAG neural networks to model Boolean constraint propagation. Other studies investigate permutation-invariant architectures for learning directly from CNF formulas (Cameron et al., 2020) or unsupervised end-to-end frameworks for Weighted MaxSAT based on hypergraph neural networks (Chen et al., 2025). In contrast to these approaches, we focus on unsat-core prediction, rather than directly predicting the satis-

fiability of SAT instances. We model CNF formulas as clause-literal hypergraphs augmented with a clause-clause incidence graph, which enables the capture of higher-order relationships among literals and clauses.

Learning-Guided SAT Solving. Another line of research leverages neural networks to guide heuristics in SAT solvers, aiming to reduce the reliance on domain expertise. Most existing methods focus on CDCL solvers, with some extensions to stochastic local search (SLS). For CDCL solvers, (Liang et al., 2018) proposes a learning-based restart policy that predicts the quality of learned clauses. NeuroCore (Selsam & Bjørner, 2019) extends NeuroSAT to predict unsat-core variables and guides variable selection accordingly. Graph-Q-SAT (Kurin et al., 2020) introduces a reinforcement learning-based branching heuristic, while NeuroBack (Wang et al., 2024) improves phase selection by predicting backbone variable phases prior to solving. NeuroSelect (Liu et al., 2024) learns adaptive clause-deletion strategies using a graph transformer, and RLAF (Tönshoff & Grohe, 2025) injects learned variable weights and polarities into branching heuristics in a one-shot manner. For SLS solvers, (Yolcu & Póczos, 2019) and NLocalSAT (Zhang et al., 2020) apply GNNs to variable selection and assignment initialization, respectively, while NSNet (Li & Si, 2022) formulates SAT and #SAT as probabilistic inference and applies GNN-based belief propagation. In addition, GraSS (Zhang et al., 2024) addresses solver selection via graph-based representations. Our work follows the learning-guided paradigm for CDCL solvers by predicting unsat-core variables, and further enhances it with decomposed message passing and polarity-aware consistency regularization.

6. Conclusion

In this paper, we presented a polarity-aware hypergraph-based framework for unsat-core variable prediction in SAT problems. By modeling SAT formulas as clause-literal hypergraphs augmented with clause-level interactions, the proposed approach captures higher-order structural dependencies. The introduction of invariant-equivariant variable decomposition enables explicit modeling of the relationship between positive and negative literals, while the polarity-inversion consistency regularization further enforces intrinsic symmetry properties of SAT during training.

Experimental results across multiple datasets demonstrate that PASAT consistently improves unsat-core variable prediction over existing learning-based approaches, and offers practical benefits when integrated with CDCL solvers. Future work includes developing more expressive hypergraph-based representations for SAT formulas and extending the framework to a broader range of SAT problems.

Impact Statement

This paper presents work whose goal is to advance the field of Machine Learning. There are many potential societal consequences of our work, none which we feel must be specifically highlighted here.

References

- Amizadeh, S., Matuselych, S., and Weimer, M. Learning to solve circuit-sat: An unsupervised differentiable approach. In *7th International Conference on Learning Representations, ICLR 2019, New Orleans, LA, USA, May 6-9, 2019*. OpenReview.net, 2019.
- Audemard, G. and Simon, L. Glucose and syrup in the sat competition 2017. In *Proceedings of SAT Competition 2017*, 2017.
- Bai, S., Zhang, F., and Torr, P. H. S. Hypergraph convolution and hypergraph attention. *Pattern Recognit.*, 110:107637, 2021. doi: 10.1016/J.PATCOG.2020.107637.
- Biere, A., Heule, M., van Maaren, H., and Walsh, T. (eds.). *Handbook of Satisfiability - Second Edition*, volume 336 of *Frontiers in Artificial Intelligence and Applications*. IOS Press, 2021. ISBN 978-1-64368-160-3. doi: 10.3233/FAIA336.
- Bünz, B. and Lamm, M. Graph neural networks and boolean satisfiability. *CoRR*, abs/1702.03592, 2017.
- Büttner, M. and Rintanen, J. Satisfiability planning with constraints on the number of actions. In Biundo, S., Myers, K. L., and Rajan, K. (eds.), *Proceedings of the Fifteenth International Conference on Automated Planning and Scheduling (ICAPS 2005), June 5-10 2005, Monterey, California, USA*, pp. 292–299. AAAI, 2005.
- Cameron, C., Chen, R., Hartford, J. S., and Leyton-Brown, K. Predicting propositional satisfiability via end-to-end learning. In *The Thirty-Fourth AAAI Conference on Artificial Intelligence, AAAI 2020, The Thirty-Second Innovative Applications of Artificial Intelligence Conference, IAAI 2020, The Tenth AAAI Symposium on Educational Advances in Artificial Intelligence, EAAI 2020, New York, NY, USA, February 7-12, 2020*, pp. 3324–3331. AAAI Press, 2020.
- Chen, Q., Tan, S., Gao, S., and Lü, J. Hypersat: Unsupervised hypergraph neural networks for weighted maxsat problems. *CoRR*, abs/2504.11885, 2025. doi: 10.48550/ARXIV.2504.11885.
- Cook, S. A. The complexity of theorem-proving procedures. In Harrison, M. A., Banerji, R. B., and Ullman, J. D. (eds.), *Proceedings of the 3rd Annual ACM Symposium on Theory of Computing, May 3-5, 1971, Shaker Heights, Ohio, USA*, pp. 151–158. ACM, 1971. doi: 10.1145/800157.805047.
- Feng, Y., You, H., Zhang, Z., Ji, R., and Gao, Y. Hypergraph neural networks. In *The Thirty-Third AAAI Conference on Artificial Intelligence, AAAI 2019, The Thirty-First Innovative Applications of Artificial Intelligence Conference, IAAI 2019, The Ninth AAAI Symposium on Educational Advances in Artificial Intelligence, EAAI 2019, Honolulu, Hawaii, USA, January 27 - February 1, 2019*, pp. 3558–3565. AAAI Press, 2019. doi: 10.1609/AAAI.V33I01.33013558.
- Giráldez-Cru, J. and Levy, J. A modularity-based random SAT instances generator. In Yang, Q. and Wooldridge, M. J. (eds.), *Proceedings of the Twenty-Fourth International Joint Conference on Artificial Intelligence, IJCAI 2015, Buenos Aires, Argentina, July 25-31, 2015*, pp. 1952–1958. AAAI Press, 2015.
- Giráldez-Cru, J. and Levy, J. A modularity-based random sat instances generator. In *IJCAI*, volume 15, pp. 1952–1958, 2015.
- Hamilton, W. L., Ying, Z., and Leskovec, J. Inductive representation learning on large graphs. In Guyon, I., von Luxburg, U., Bengio, S., Wallach, H. M., Fergus, R., Vishwanathan, S. V. N., and Garnett, R. (eds.), *Advances in Neural Information Processing Systems 30: Annual Conference on Neural Information Processing Systems 2017, December 4-9, 2017, Long Beach, CA, USA*, pp. 1024–1034, 2017.
- Kipf, T. N. and Welling, M. Semi-supervised classification with graph convolutional networks. In *5th International Conference on Learning Representations, ICLR, 2016*.
- Kullback, S. and Leibler, R. A. On information and sufficiency. *The annals of mathematical statistics*, 22(1): 79–86, 1951.
- Kurin, V., Godil, S., Whiteson, S., and Catanzaro, B. Can q-learning with graph networks learn a generalizable branching heuristic for a SAT solver? In Larochelle, H., Ranzato, M., Hadsell, R., Balcan, M., and Lin, H. (eds.), *Advances in Neural Information Processing Systems 33: Annual Conference on Neural Information Processing Systems 2020, NeurIPS 2020, December 6-12, 2020, virtual*, 2020.
- Li, M., Shi, Z., Lai, Q., Khan, S., Cai, S., and Xu, Q. On eda-driven learning for SAT solving. In *60th ACM/IEEE Design Automation Conference, DAC 2023, San Francisco, CA, USA, July 9-13, 2023*, pp. 1–6. IEEE, 2023. doi: 10.1109/DAC56929.2023.10248001.

- Li, Z. and Si, X. Nsnet: A general neural probabilistic framework for satisfiability problems. In Koyejo, S., Mohamed, S., Agarwal, A., Belgrave, D., Cho, K., and Oh, A. (eds.), *Advances in Neural Information Processing Systems 35: Annual Conference on Neural Information Processing Systems 2022, NeurIPS 2022, New Orleans, LA, USA, November 28 - December 9, 2022*, 2022.
- Li, Z., Guo, J., and Si, X. G4satbench: Benchmarking and advancing SAT solving with graph neural networks. *Trans. Mach. Learn. Res.*, 2024, 2024.
- Liang, J. H., Oh, C., Mathew, M., Thomas, C., Li, C., and Ganesh, V. Machine learning-based restart policy for CDCL SAT solvers. In Beyersdorff, O. and Wintersteiger, C. M. (eds.), *Theory and Applications of Satisfiability Testing - SAT 2018 - 21st International Conference, SAT 2018, Held as Part of the Federated Logic Conference, FloC 2018, Oxford, UK, July 9-12, 2018, Proceedings*, volume 10929 of *Lecture Notes in Computer Science*, pp. 94–110. Springer, 2018. doi: 10.1007/978-3-319-94144-8_6.
- Liu, H., Xu, P., Pu, Y., Yin, L., Zhen, H., Yuan, M., Ho, T., and Yu, B. Neuroselect: Learning to select clauses in SAT solvers. In De, V. (ed.), *Proceedings of the 61st ACM/IEEE Design Automation Conference, DAC 2024, San Francisco, CA, USA, June 23-27, 2024*, pp. 131:1–131:6. ACM, 2024. doi: 10.1145/3649329.3656250.
- Mironov, I. and Zhang, L. Applications of SAT solvers to cryptanalysis of hash functions. In Biere, A. and Gomes, C. P. (eds.), *Theory and Applications of Satisfiability Testing - SAT 2006, 9th International Conference, Seattle, WA, USA, August 12-15, 2006, Proceedings*, volume 4121 of *Lecture Notes in Computer Science*, pp. 102–115. Springer, 2006. doi: 10.1007/11814948_13.
- Selsam, D. and Bjørner, N. S. Guiding high-performance SAT solvers with unsat-core predictions. In Janota, M. and Lynce, I. (eds.), *Theory and Applications of Satisfiability Testing - SAT 2019 - 22nd International Conference, SAT 2019, Lisbon, Portugal, July 9-12, 2019, Proceedings*, volume 11628 of *Lecture Notes in Computer Science*, pp. 336–353. Springer, 2019. doi: 10.1007/978-3-030-24258-9_24.
- Selsam, D., Lamm, M., Bünz, B., Liang, P., de Moura, L., and Dill, D. L. Learning a SAT solver from single-bit supervision. In *7th International Conference on Learning Representations, ICLR 2019, New Orleans, LA, USA, May 6-9, 2019*. OpenReview.net, 2019.
- Shi, Z., Li, M., Liu, Y., Khan, S., Huang, J., Zhen, H., Yuan, M., and Xu, Q. Satformer: Transformer-based UNSAT core learning. In *IEEE/ACM International Conference on Computer Aided Design, ICCAD 2023, San Francisco, CA, USA, October 28 - Nov. 2, 2023*, pp. 1–4. IEEE, 2023. doi: 10.1109/ICCAD57390.2023.10323731.
- Tönshoff, J. and Grohe, M. Learning from algorithm feedback: One-shot SAT solver guidance with gnns. *CoRR*, abs/2505.16053, 2025. doi: 10.48550/ARXIV.2505.16053.
- Vizel, Y., Weissenbacher, G., and Malik, S. Boolean satisfiability solvers and their applications in model checking. *Proc. IEEE*, 103(11):2021–2035, 2015. doi: 10.1109/JPROC.2015.2455034.
- Wang, W., Hu, Y., Tiwari, M., Khurshid, S., McMillan, K. L., and Miikkulainen, R. Neuroback: Improving CDCL SAT solving using graph neural networks. In *The Twelfth International Conference on Learning Representations, ICLR 2024, Vienna, Austria, May 7-11, 2024*. OpenReview.net, 2024.
- Yolcu, E. and Póczos, B. Learning local search heuristics for boolean satisfiability. In Wallach, H. M., Larochelle, H., Beygelzimer, A., d’Alché-Buc, F., Fox, E. B., and Garnett, R. (eds.), *Advances in Neural Information Processing Systems 32: Annual Conference on Neural Information Processing Systems 2019, NeurIPS 2019, December 8-14, 2019, Vancouver, BC, Canada*, pp. 7990–8001, 2019.
- Zhang, W., Sun, Z., Zhu, Q., Li, G., Cai, S., Xiong, Y., and Zhang, L. Nlocalsat: Boosting local search with solution prediction. In Bessiere, C. (ed.), *Proceedings of the Twenty-Ninth International Joint Conference on Artificial Intelligence, IJCAI 2020*, pp. 1177–1183. ijcai.org, 2020. doi: 10.24963/IJCAI.2020/164.
- Zhang, Z., Chételat, D., Cotnareanu, J., Ghose, A., Xiao, W., Zhen, H., Zhang, Y., Hao, J., Coates, M., and Yuan, M. Grass: Combining graph neural networks with expert knowledge for SAT solver selection. In Baeza-Yates, R. and Bonchi, F. (eds.), *Proceedings of the 30th ACM SIGKDD Conference on Knowledge Discovery and Data Mining, KDD 2024, Barcelona, Spain, August 25-29, 2024*, pp. 6301–6311. ACM, 2024. doi: 10.1145/3637528.3671627.

A. Dataset Details

In unsat-core prediction tasks, we use three generated SAT datasets, namely SR, Community Attachment (CA), and Popularity-Similarity (PS), following the dataset construction procedure of G4SATBench (Li et al., 2024). Specifically, CNF formulas are generated using the SR generator from NeuroSAT (Selsam et al., 2019), the Community Attachment (CA) model (Giráldez-Cru & Levy, 2015), and the Popularity-Similarity (PS) model (Giráldez-Cru & Levy, 2015). Each dataset is divided into three difficulty levels: easy, medium, and hard. For each difficulty level, the training set contains 80,000 pairs of satisfiable and unsatisfiable instances, while the validation and test sets each contain 10,000 such pairs. For the unsat-core prediction task, we use only unsatisfiable instances for both training and evaluation, following the same setting as NeuroSAT (Selsam et al., 2019). The detailed statistics of these datasets are summarized in Table 4.

Table 4. Statistics of datasets with difficulty splits.

DATASET	SPLIT	VARIABLES			CLAUSES			UNSAT-CORE VARS		
		AVG.	MIN	MAX	AVG.	MIN	MAX	AVG.	MIN	MAX
SR	EASY	24.99	10	40	148.32	23	355	19.64	2	40
	MEDIUM	120.11	40	200	654.81	128	1332	99.49	2	200
	HARD	300.10	200	400	1616.47	420	2449	277.83	3	400
CA	EASY	30.39	16	40	278.67	57	590	5.74	4	40
	MEDIUM	119.60	40	200	1651.41	162	2999	17.16	4	118
	HARD	299.93	200	400	4197.51	2601	5998	42.19	19	146
PS	EASY	27.25	10	40	192.22	54	319	18.86	3	40
	MEDIUM	123.48	40	200	869.65	224	1599	65.86	3	200
	HARD	250.17	200	300	1761.98	917	2399	127.02	3	300

In Exp-4, we construct the training data using instances from the SAT Competition Main Track spanning 2017 to 2022, following the data generation procedure for unsat core variable prediction described in (Selsam & Bjørner, 2019). Instances from the SAT Competition Main Track in 2023 to 2025 are reserved exclusively for solver evaluation. During evaluation, the trained model predicts variable scores for each instance, which are used to guide variable selection in the Glucose solver. Statistics of the training and evaluation datasets are summarized in Table 5.

Table 5. Statistics of SAT Competition Main Track instances.

YEAR	#INST.	STATUS		VARIABLES				CLAUSES			
		SAT	UNSAT	AVG.	MED.	MIN	MAX	AVG.	MED.	MIN	MAX
SATCOMP 2017	350	133	140	521955.61	7411.5	180	8905808	1879089.81	138764.0	648	32322587
SATCOMP 2018	400	192	134	360371.86	29690.0	175	3171415	1646869.57	248471.0	1119	17708937
SATCOMP 2019	399	161	128	247171.81	8591.0	97	9582411	1562906.69	117206.0	204	103690720
SATCOMP 2020	400	191	145	310404.10	30999.5	54	8043699	4007261.77	274643.0	58	129333040
SATCOMP 2021	400	156	187	192789.42	24062.0	44	3416996	2733968.29	236609.5	513	67009046
SATCOMP 2022	400	172	186	981553.01	34939.0	99	18707849	7117471.09	292902.0	264	214309011
SATCOMP 2023	400	154	219	911146.56	11636.5	45	21185701	4477681.16	81176.5	376	96368706
SATCOMP 2024	400	179	208	1435523.72	4566.5	74	48505464	5028755.65	62239.5	252	130975382
SATCOMP 2025	400	96	80	1588632.13	24367.0	149	117295030	6015936.93	259340.0	606	315573317

B. Detailed Experimental Settings

B.1. Implementation Details and Hyperparameters

All methods are implemented using PyTorch². The experiments are conducted on a workstation equipped with an Intel Xeon Gold 6148 CPU at 2.40 GHz and an NVIDIA Tesla V100 PCIe GPU with 32 GB memory. The GPU is used for training and evaluating neural models, while the CPU is used for data processing and solving SAT instances with classical solvers. The hyperparameter settings used in our experiments are summarized in Table 6.

²<https://pytorch.org/>

Table 6. Hyperparameter settings used in our experiments.

HYPERPARAMETER	VALUE RANGE / SET
HIDDEN DIMENSION	80
MESSAGE PASSING ROUNDS (T)	{2, 4}
MLP LAYERS	{2, 3}
EPOCHS	{100, 200}
BATCH SIZE	{100, 200}
LEARNING RATE	{1E-4, 2E-4, 4E-4}
WEIGHT DECAY	{1E-4, 5E-4}
GRADIENT CLIPPING	{1, 2, 5, 10}
LR SCHEDULER	EXPONENTIALLR
LR DECAY FACTOR (γ)	{0.871, 0.95}
CONSISTENCY WEIGHT (λ_{cons})	{0.1, 0.3}
DECOMPOSITION WEIGHT (λ_{decomp})	{0.05, 0.15}

B.2. SAT Solver Integration Details

In Exp-4, we follow the training and evaluation pipeline proposed in NeuroCore (Selsam & Bjørner, 2019). We first generate training data using SAT Competition Main Track instances from 2017 to 2022, following the same data construction procedure. For each year, we generate 20,000 training samples. The resulting dataset is used to train our neural model for unsat core variable prediction. The training settings are the same as in the previous experiments. After training, the model is applied to SAT Competition Main Track instances from 2023 to 2025 to predict unsat core variable scores for each instance.

In contrast to NeuroCore, we modify the Glucose solver to accept both the CNF formula and the predicted variable scores as input. We use Glucose release 4.2.1 as the base solver. During solving, each instance is limited to a time budget of 5000 seconds. The modified solver periodically updates variable activity scores every 100 seconds by overwriting them with the predicted variable scores, thereby guiding variable selection during solving. To satisfy GPU memory constraints during inference, we restrict the maximum problem size processed by the neural model. Specifically, the total number of literals and variables is limited to at most 300,000, and the number of literal–clause incidence relations is limited to at most 2,000,000, similar to the data limits used in NeuroCore. In addition, when constructing the clause–clause graph, we retain only the top-50 weighted edges for each clause, corresponding to the strongest inter-clause relationships.